Production of a $_\Lambda^4$He hypernucleus in the ^{4}He(π, K) reactions reexamined

Toru Harada[1,2,*] and Yoshiharu Hirabayashi[3]

[1]*Center for Physics and Mathematics, Osaka Electro-Communication University, Neyagawa, Osaka 572-8530, Japan*
[2]*J-PARC Branch, KEK Theory Center, Institute of Particle and Nuclear Studies,*
High Energy Accelerator Research Organization (KEK), 203-1 Shirakata, Tokai, Ibaraki 319-1106, Japan
[3]*Information Initiative Center, Hokkaido University, Sapporo 060-0811, Japan*

We investigate theoretically production cross sections of the $J^\pi = 0^+$ ground state of a $_\Lambda^4$He hypernucleus in the ^{4}He(π, K) reaction with a distorted-wave impulse approximation using the optimal Fermi-averaged $\pi N \to K\Lambda$ t matrix. We demonstrate the sensitivity of the production cross sections to the Λ wave functions obtained from $3N$-Λ potentials and to meson distorted waves in eikonal distortions. It is shown that the calculated laboratory cross sections of the 0^+ ground state in $_\Lambda^4$He amount to $(d\sigma/d\Omega)_{lab} \simeq 11$ μb/sr at $p_\pi = 1.05$ GeV/c in the K forward direction because of an advantage of the use of an s-shell target nucleus such as ^{4}He. The importance of the recoil effects and the energy dependence of the $\pi N \to K\Lambda$ cross sections is also discussed.

I. INTRODUCTION

Recently, unexpected short lifetimes of a $_\Lambda^3$H hypernucleus were measured in hypernuclear production of high-energy heavy-ion collisions [1–3]; the world average lifetime of $\tau^{(av)}(_\Lambda^3$H$) = 185^{+23}_{-28}$ ps is shorter than the free lifetime $\tau_\Lambda = 263.2 \pm 2.0$ ps by about 30%. However, the ALICE Collaboration [4] recently reported the result $\tau(_\Lambda^3$H$) = 237^{+33}_{-36}$ ps, which is moderately closer to τ_Λ. This is one of the most topical issues to study in hypernuclear physics [5] and is essential because $_\Lambda^3$H is the lightest hypernucleus which provides valuable information on interactions of a Λ hyperon with nucleons [6]. In addition, the HypHI Collaboration [1] suggested that the lifetime of a $_\Lambda^4$H hypernucleus, $\tau(_\Lambda^4$H$) = 140^{+48}_{-33}$ ps, is shorter than the $\tau(_\Lambda^4$H$) = 194^{+28}_{-26}$ ps measured in stopped K^- experiments at KEK [7], whereas theoretical calculations [8,9] predicted $\tau(_\Lambda^4$H$) = 196$-264 ps, which depends on the Λ wave functions. To solve the lifetime puzzle, experimental measurements of the $_\Lambda^{3,4}$H lifetime have been planned in (K^-, π^0) and (π^-, K^0) reactions on ^{3,4}He targets at J-PARC [10,11]. Therefore, it is important to investigate theoretically the production of $A = 3$, 4 hypernuclei via ($\bar{K}$, π) and (π, K) reactions on ^{3,4}He targets [12]. Especially, we believe that Λ production studies on the ^{4}He target are useful for settling mysterious problems related to the $A = 4$ hypernuclei [13], e.g., the overbinding/underbinding anomaly [14,15] and charge symmetry breaking [16,17].

Many theoretical studies of hypernuclear spectroscopy have been performed in nuclear (K^-, π^-), (π^+, K^+), and (γ, K^+) reactions [13]. Production cross sections of Λ hypernuclear states for each reaction are usually characterized by a specific momentum transfer to a Λ hyperon. The

(K^-, π^-) reactions on ^{4}He [18] can produce a Λ substitutional state in $_\Lambda^4$He under recoilless conditions. On the other hand, the (π^+, K^+) reactions on ^{4}He enable us to make large momentum transfers of $q = 300$–500 MeV/c [19], populating a Λ stretched state which seems to be disadvantageous to the $0s_N \to 0s_\Lambda$ transition in terms of a momentum matching law [20]; however, the production cross sections of $_\Lambda^4$He via the (π^+, K^+) reaction on ^{4}He were predicted theoretically [21] for the nonmesonic weak decay of $_\Lambda^4$He and $_\Lambda^4$H at J-PARC [22]. Consequently, it is worth revisiting investigation of $_\Lambda^4$He production via the (π, K) reactions on ^{4}He because we have now achieved a good understanding of nuclear (π, K) reactions [23].

In this paper, we investigate theoretically the production cross sections of the $J^\pi = 0^+$ ground state ($0^+_{g.s.}$) of a $_\Lambda^4$He hypernucleus via the ^{4}He(π^+, K^+) reaction in the distorted-wave impulse approximation. We demonstrate the differential cross sections at $p_\pi = 1.05$ GeV/c in the K^+ forward direction in the laboratory system. We discuss medium effects of the $\pi N \to K\Lambda$ amplitude in nuclear (π, K) reactions and recoil effects in a light hypernucleus such as $_\Lambda^4$He. Our results on $_\Lambda^4$He production via ^{4}He(π^+, K^+) reactions are expected to be identical to those on $_\Lambda^4$H mirror production via ^{4}He(π^-, K^0) reactions because charge independence guarantees $f_{\pi^+ n \to K^+ \Lambda} = -f_{\pi^- p \to K^0 \Lambda}$ in the (π, K) reactions on $T = 0$ target nuclei.

II. CALCULATIONS

A. Distorted-wave impulse approximation

Let us consider a calculation procedure of hypernuclear production for nuclear (π, K) reactions in the laboratory frame. The double-differential cross sections within the distorted-wave impulse approximation (DWIA) [24,25] are

---

024605-1

given by (in units of $\hbar = c = 1$)

$$\frac{d^2\sigma}{dE_K d\Omega_K} = \beta \frac{1}{[J_A]} \sum_{m_A} \sum_{B,m_B} |\langle \Psi_B | \hat{F} | \Psi_A \rangle|^2$$

$$\times \delta(E_K + E_B - E_\pi - E_A), \qquad (1)$$

where $[J] = 2J + 1$, and E_K, E_π, E_B, and E_A are the energies of outgoing K, incoming π, hypernuclear states, and the target nucleus, respectively. Ψ_B and Ψ_A are wave functions of hypernuclear final states and the initial state of the target nucleus, respectively. The kinematical factor β [26,27] arising from a translation from a two-body meson-nucleon laboratory system to a meson-nucleus laboratory system [28] is given by

$$\beta = \left(1 + \frac{E_K^{(0)}}{E_B^{(0)}} \frac{p_K^{(0)} - p_\pi^{(0)} \cos\theta_{\text{lab}}}{p_K^{(0)}}\right) \frac{p_K E_K}{p_K^{(0)} E_K^{(0)}}, \qquad (2)$$

where $p_\pi^{(0)}$ and $p_K^{(0)}$ [$E_K^{(0)}$ and $E_B^{(0)}$] are laboratory momenta of π and K (laboratory energies of K and Λ) in the two-body $\pi N \to K\Lambda$ reaction, respectively. Here we have considered only the non-spin-flip amplitude because we are interested in the $\Delta S = 0$ cross sections in the K forward direction. Thus an external operator $\hat{F}$ for the associated production $\pi N \to K\Lambda$ reactions is given by

$$\hat{F} = \int d\mathbf{r} \, \chi_K^{(-)*}(\mathbf{p}_K, \mathbf{r}) \chi_\pi^{(+)}(\mathbf{p}_\pi, \mathbf{r}) \sum_{j=1}^{A} \overline{f}_{\pi N \to K\Lambda} \delta(\mathbf{r} - \mathbf{r}_j) \hat{O}_j,$$

$$(3)$$

where we assume zero-range interaction for the $\pi N \to K\Lambda$ transitions. Distorted waves of $\chi_K^{(-)*}$ and $\chi_\pi^{(+)}$ are obtained with the help of the eikonal approximation [24]. $\hat{O}_j$ is a baryon operator changing the jth nucleon into a Λ hyperon in the nucleus, and $\mathbf{r}$ is the relative coordinate between the mesons and the center-of-mass (c.m.) of the nucleus; $\overline{f}_{\pi N \to K\Lambda}$ is the Fermi-averaged non-spin-flip amplitude for the $\pi N \to K\Lambda$ reactions in nuclei in the laboratory frame [23].

The energy and momentum transfer to the Λ final state is given by

$$\omega = E_\pi - E_K, \quad \mathbf{q} = \mathbf{p}_\pi - \mathbf{p}_K, \qquad (4)$$

where $E_\pi = (m_\pi^2 + \mathbf{p}_\pi^2)^{1/2}$ and $E_K = (m_K^2 + \mathbf{p}_K^2)^{1/2}$ are the laboratory energies of π and K in the nuclear reaction, respectively; m_π and m_K ($\mathbf{p}_\pi$ and $\mathbf{p}_K$) are the masses (laboratory momenta) of π and K, respectively. Figure 1 displays the momentum transfer to the $0^+_{\text{g.s.}}$ final state in $^4_\Lambda$He,

$$q = \left(p_\pi^2 + p_K^2 - 2 p_\pi p_K \cos\theta_{\text{lab}}\right)^{1/2}, \qquad (5)$$

as a function of the incident laboratory momentum p_π.

The differential laboratory cross section of a Λ hypernuclear state is obtained by the energy integration [29]

$$\left(\frac{d\sigma}{d\Omega_K}\right) = \int dE_K \left(\frac{d^2\sigma}{dE_K d\Omega_K}\right) \qquad (6)$$

around a corresponding peak in the inclusive K spectrum. We often incorporate the effective number technique into the differential laboratory cross section within the DWIA [24,
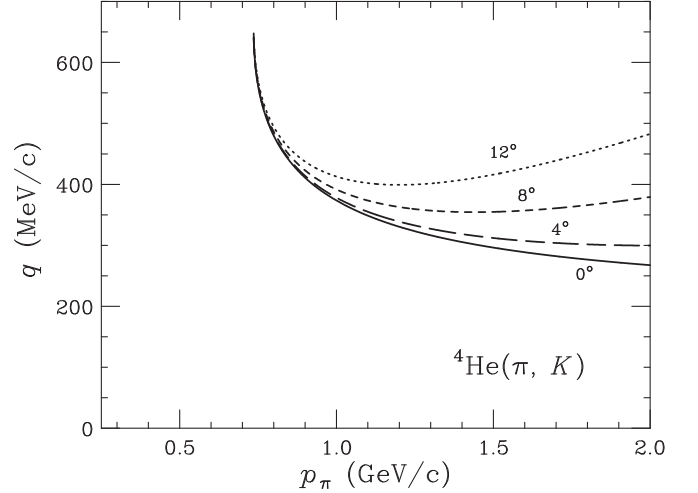

FIG. 1. Momentum transfer q to the Λ final state of $0^+_{\text{g.s.}}$ in $^4_\Lambda$He for (π, K) reactions on a ^{4}He target at K forward-direction angles of $\theta_{\text{lab}} = 0°$-$12°$ in the laboratory frame, as a function of the incident laboratory momentum p_π.

27–30]. Thus the differential laboratory cross section of the Λ bound state with J^π can be written as

$$\left(\frac{d\sigma}{d\Omega_K}\right)^{J^\pi}_{\text{lab},\theta_{\text{lab}}} = \alpha \frac{1}{[J_A]} \sum_{m_A m_B} |\langle \Psi_B | \overline{f}_{\pi N \to K\Lambda}$$

$$\times \chi_K^{(-)*}\left(\mathbf{p}_K, \frac{M_C}{M_B}\mathbf{r}\right) \chi_\pi^{(+)}\left(\mathbf{p}_\pi, \frac{M_C}{M_A}\mathbf{r}\right) |\Psi_A\rangle|^2,$$

$$(7)$$

where $\mathbf{r}$ is the relative coordinate between a $3N$-core nucleus and a nucleon or Λ hyperon; the factors M_C/M_B and M_C/M_A take into account the recoil effects, where M_A, M_B, and M_C are the masses of the target, the hypernucleus, and the core nucleus, respectively. The kinematical factor α [28] is related to β in Eq. (2) as

$$\alpha = \beta \left(1 + \frac{E_K}{E_B} \frac{p_K - p_\pi \cos\theta_{\text{lab}}}{p_K}\right)^{-1}. \qquad (8)$$

In Table I, we list the kinematic values for $^4_\Lambda$He production via the nuclear (π, K) reaction on a ^{4}He target at $p_\pi = 1.05$ GeV/c, $\theta_{\text{lab}} = 0°$, $4°$, $8°$, and $12°$, where we choose $B_\Lambda = 2.39$ MeV as the Λ binding energy for $0^+_{\text{g.s}}$ in $^4_\Lambda$He. Note that the value of α for a ^{4}He target at $p_\pi = 1.05$ GeV/c ($0°$) amounts to 0.828, which is 25% larger than that for heavier nuclei; $\alpha \simeq 0.66$ for a ^{40}Ca target [20].

B. Fermi-averaged (π, K) cross sections

It should be noted that a strong energy dependence of differential laboratory cross sections appears in the nuclear (π, K) reactions, as discussed in Ref. [23]. To consider the p_π dependence of elementary $\pi N \to K\Lambda$ laboratory cross sections, we average the $\pi N \to K\Lambda$ t matrix in the laboratory frame over a Fermi-momentum distribution, where nuclear effects of a nucleon binding ε_N are naturally taken into account. This procedure is called "optimal Fermi averaging" under the

TABLE I. Kinematical values and $\pi N \to K\Lambda$ laboratory cross sections in nuclear (π, K) reactions on a ^{4}He target at $p_\pi = 1.05$ GeV/c. The non-spin-flip amplitudes in the $\pi N \to K\Lambda$ reaction are used.

$\theta_{\rm lab}$	p_K	q	$q_{\rm eff}$[a]	β	α	$\alpha \langle d\sigma/d\Omega \rangle_{\pi N \to \Lambda K}$	
(deg)	(MeV/c)	(MeV/c)	(MeV/c)			Free (μb/sr)	Opt. (μb/sr)
0	690.1	359.9	271.1	0.684	0.828	574	464
4	689.5	365.4	275.3	0.686	0.829	561	487
8	687.7	381.3	287.3	0.692	0.834	525	468
12	684.6	406.2	306.1	0.703	0.843	472	416

[a]Effective momentum transfer to the Λ final state, $q_{\rm eff} \approx (M_{\rm C}/M_{\rm A})q$, given in Eq. (30).

on-energy-shell condition [23]. Charge independence guarantees the following relation between the $\pi N \to K\Lambda$ amplitudes:

$$f_{\pi^+ n \to K^+ \Lambda} = -f_{\pi^- p \to K^0 \Lambda}. \qquad (9)$$

Thus the (π^+, K^+) and (π^-, K^0) cross sections are identical to each other on the $T = 0$ nuclear targets as ^{4}He. Here we have employed the elementary $\pi^- p \to K^0 \Lambda$ amplitudes analyzed by Sotona and Žofka [31].

Figure 2 shows the optimal Fermi-averaged $\pi N \to K\Lambda$ laboratory cross sections of $\alpha \langle d\sigma/d\Omega \rangle^{\rm opt}_{\pi N \to K\Lambda}$ including the kinematical factor α in nuclear (π, K) reactions on a ^{4}He target, together with the elementary $\pi N \to K\Lambda$ laboratory cross sections of $\alpha \langle d\sigma/d\Omega \rangle^{\rm free}_{\pi N \to K\Lambda}$ in free space [31]. The peaks of $\alpha \langle d\sigma/d\Omega \rangle^{\rm free}_{\pi N \to K\Lambda}$ are located at $p_\pi \simeq 1.05$ GeV/c, corresponding to $M(\pi N) \simeq 1700$ MeV/c^2 in the invariant mass of π and N, because there exist N^* resonances, e.g., $S_{11}(1680)$, $P_{11}(1730)$, and $P_{13}(1700)$. We find that the peaks of $\alpha \langle d\sigma/d\Omega \rangle^{\rm opt}_{\pi N \to K\Lambda}$ are shifted to the position of $p_\pi \simeq 1.00$ GeV/c, taking into account the Fermi motion of a struck nucleon under the optimal condition in the nucleus; the
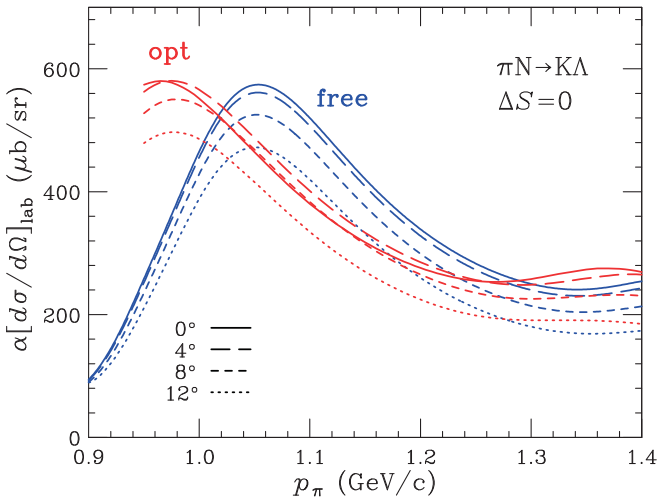

FIG. 2. Optimal Fermi-averaged $\pi N \to K\Lambda$ laboratory cross sections of $\alpha \langle d\sigma/d\Omega_K \rangle^{\rm opt}_{\pi N \to K\Lambda}$ for the $\Delta S = 0$ nuclear (π, K) reactions in nuclei [23], as a function of the incident laboratory momentum p_π. The kinematics for a ^{4}He target and the non-spin-flip amplitude at K forward-direction laboratory angles of $\theta_{\rm lab}$ are used. Elementary $\pi N \to K\Lambda$ laboratory cross sections of $\alpha \langle d\sigma/d\Omega_K \rangle^{\rm free}_{\pi N \to K\Lambda}$ for $\Delta S = 0$ in free space [31] are also drawn.

shape of $\alpha \langle d\sigma/d\Omega \rangle^{\rm opt}_{\pi N \to K\Lambda}$ is moderately broader than that of $\alpha \langle d\sigma/d\Omega \rangle^{\rm free}_{\pi N \to K\Lambda}$. In Table I, we also list the values of $\alpha \langle d\sigma/d\Omega \rangle^{\rm opt}_{\pi N \to \Lambda K}$, together with the kinematical factor α at $p_\pi = 1.05$ GeV/c.

C. Wave functions

In our calculations, we have assumed the 3N 1/2$^+$ ground state as a core nucleus in $A = 4$ systems [18], i.e., ϕ_{3N} is a wave function for the 3N eigenstates (^{3}He or ^{3}H), and we have neglected the charge symmetry-breaking effects in $A = 4$ hypernuclei. Thus the wave function of the 0$^+$ ground state $(0^+_{\rm g.s.})$ in $^4_\Lambda$He ($L_B = 0$, $S_B = 0$, $T_B = 1/2$) is written as

$$\Psi_B = \left[\left[\phi_{3N} \otimes \varphi^{(\Lambda)}_{\ell_\Lambda}\right]_{L_B} \otimes X^B_{T_B, S_B}\right]_{J_B},$$
$$X^B_{T_B, S_B} = \left[\chi^{(3N)}_{I_3, S_3} \otimes \chi^{(\Lambda)}_{0, 1/2}\right]_{1/2, 0}, \qquad (10)$$

where $\varphi^{(\Lambda)}_{\ell_\Lambda}$ is a relative wave function between 3N and Λ, and $X^B_{T_B, S_B}$ is the isospin-spin function for 0$^+_{\rm g.s.}$ in $^4_\Lambda$He; $\chi^{(3N)}_{I_3, S_3}$ and $\chi^{(\Lambda)}_{0, 1/2}$ are the isospin-spin functions for 3N (isospin I_3, spin S_3) and Λ ($I = 0$, $S = 1/2$), respectively. The explicit form of $X^B_{T_B, S_B}$ is given in the Appendix. According to Ref. [32], we use $\varphi^{(\Lambda)}_{\ell_\Lambda}$, which is regarded as a spectroscopic amplitude obtained from a four-body ΛNNN wave function using realistic central nucleon-nucleon (NN) and ΛN potentials [14]. It should be noted that $\varphi^{(\Lambda)}_{\ell_\Lambda}$ includes the contribution of the ΛN short-range correlations and also many-body correlations. Thus we consider that $\varphi^{(\Lambda)}_{\ell_\Lambda}$ satisfies the Schrödinger equation

$$\left(-\frac{\hbar^2}{2\mu}\nabla^2 + U_\Lambda\right)\varphi^{(\Lambda)}_{\ell_\Lambda} = -B_\Lambda \varphi^{(\Lambda)}_{\ell_\Lambda}, \qquad (11)$$

where μ is the 3N-Λ reduced mass and B_Λ is the Λ binding energy with respect to the ^{3}He-Λ threshold. The 3N-Λ potential U_Λ is defined as

$$U_\Lambda = \langle \phi_{3N} | \bar{V}^{\rm ex} \hat{F}^{\rm ex} | \phi_{3N} \rangle, \qquad (12)$$

where $\bar{V}^{\rm ex}$ is the sum of isospin-spin averaged ΛN potentials, and $\hat{F}^{\rm ex}$ is an external operator on the basis of multiple scattering processes [33],

$$\hat{F}^{\rm ex} = 1 + \frac{Q}{e}\bar{V}^{\rm ex}\hat{F}^{\rm ex}, \qquad (13)$$

where $Q = 1 - |\phi_{3N})(\phi_{3N}|$ and $e = E - \hat{H}_{3N} + \hbar^2\nabla^2/2\mu$. Therefore, U_Λ can be derived from the four-body ΛNNN

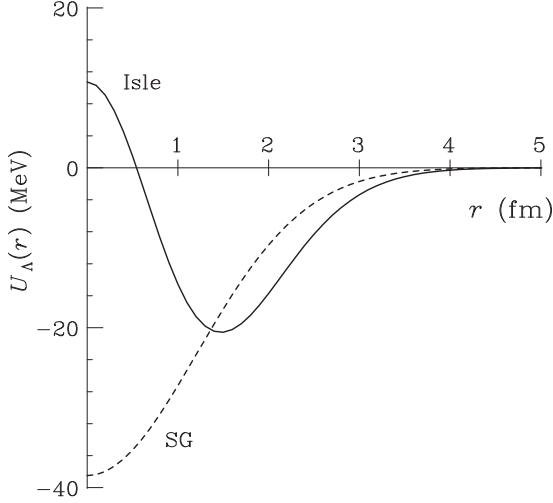FIG. 3. The $3N$-Λ potential U_Λ for $0^+_{\text{g.s.}}$ in $^4_\Lambda$He as a function of the relative distance between $3N$ and Λ. Solid and dashed curves denote the Isle and SG potentials, respectively.

FIG. 4. The $3N$-Λ density distributions $\rho_\Lambda(r)$ for $0^+_{\text{g.s.}}$ in $^4_\Lambda$He as a function of the relative distance, together with the $3N$-N density distributions $\rho_N(r)$ for $0^+_{\text{g.s.}}$ in ^{4}He. Solid and dashed curves for Λ denote the distributions for the Isle and SG potentials, respectively. The solid curve for N denotes the distribution for the C3G potential. Dotted curves represent the distributions for HO with the c.m. corrections.

wave function, taking into account the ΛN short-range correlations [32,33].

Figure 3 shows U_Λ as a function of the distance between $3N$ and Λ. We recognize that this potential has a central repulsion and an attractive tail, so we call it the "Isle" potential [9,32–34]; the central repulsion originates predominantly from the ΛN short-range correlations due to the repulsive core of the ΛN potentials, and it plays an important role in describing the lifetime of $^4_\Lambda$He in precise experimental studies on the mesonic weak decay of $\Lambda \to p\pi^-$ [7,9]. For convenience of use, we parametrize U_Λ into a two-range Gaussian form as

$$U_\Lambda(\boldsymbol{r}) = V_C \exp\{-(r/b_C)^2\} + V_A \exp\{-(r/b_A)^2\}, \quad (14)$$

where $V_C = 91.61$ MeV, $V_A = -80.88$ MeV, $b_C = 1.14$ fm, and $b_A = 1.69$ fm, reproducing the experimental data of $B_\Lambda^{\text{exp}} = 2.39 \pm 0.03$ MeV. To clearly see the effect of the central repulsion, we also introduce the single-range Gaussian (SG) potential $U_\Lambda(\boldsymbol{r}) = -38.5 \exp\{-(r/b_A)^2\}$ with $b_A = 1.70$ fm, adjusting to $B_\Lambda = 2.39$ MeV. The SG potential is often used as a phenomenological one.

The wave function of the 0^+ ground state in ^{4}He ($L_A = 0$, $S_A = 0$, $T_A = 0$) is written as

$$\Psi_A = \mathcal{A}\big[\big[\phi_{3N} \otimes \varphi^{(N)}_{\ell_N}\big]_{L_A} \otimes X^A_{T_A,S_A}\big]_{J_A},$$
$$X^A_{T_A,S_A} = \big[\chi^{(3N)}_{I_3,S_3} \otimes \chi^{(N)}_{1/2,1/2}\big]_{0,0}, \quad (15)$$

where $\mathcal{A}$ is the antisymmetrized operator for nucleons, and $\varphi^{(N)}_{\ell_N}$ is a relative wave function between $3N$ and N; $X^A_{T_A,S_A}$ and $\chi^{(N)}_{1/2,1/2}$ are the isospin-spin functions for ^{4}He and N ($I = 1/2$, $S = 1/2$), respectively. Here we have used $\varphi^{(N)}_{\ell_N}$ obtained from the $3N$-N potential U_N, which was derived from a microscopic four-body calculation with a central NN potential of Tamagaki's C3G [33]. Therefore, $\varphi^{(N)}_{\ell_N}$ includes the contribution of the NN short-range correlations and also many-body correlations [32]. For convenience of use, this
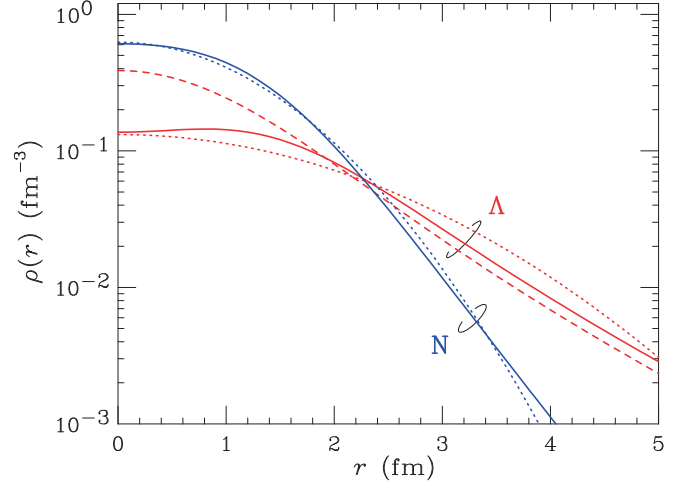
potential U_N is parametrized into useful Gaussian forms as

$$U_N(\boldsymbol{r}) = V_1 \exp\{-(r/b_1)^2\} + V_2 \exp\{-(r/b_2)^2\}$$
$$+ V_3 \exp\{-(r/b_3)^2\} \quad (16)$$

with $V_1 = 156.28$ MeV, $V_2 = -185.66$ MeV, $V_3 = -9.56$ MeV, $b_1 = 1.21$ fm, $b_2 = 1.58$ fm, and $b_3 = 2.82$ fm [35], making a fit to the experimental data of the binding energy $B_N = 20.6$ MeV and the nuclear root-mean-square (r.m.s.) distance of $\langle r_N^2 \rangle^{1/2} = 1.87$ fm between ^{3}He and n.

Figure 4 shows that $3N$-Λ density distributions $\rho_\Lambda(r)$ between $3N$ and Λ for $0^+_{\text{g.s.}}$ in $^4_\Lambda$He, as a function of the relative distance, together with $3N$-N density distributions $\rho_N(r)$ between $3N$ and N for $0^+_{\text{g.s.}}$ in ^{4}He. We find that the $3N$-Λ distribution obtained from the Isle potential differs considerably from that obtained from the SG potential around the nuclear interior; the $3N$-Λ distribution is considerably suppressed at the nuclear center, and it is pushed outside, as discussed in Refs. [32–35]. The relative r.m.s. distance between $3N$ and Λ becomes $\langle r_\Lambda^2 \rangle^{1/2} = 3.57$ fm for Isle, which is 8% larger than the 3.31 fm for SG.

To see the properties of our $\varphi^{(\Lambda)}_{\ell_\Lambda}$ obtained by U_Λ in Fig. 3, we also consider a single-particle harmonic oscillator (HO) wave function with the size parameter $b_\Lambda = (\hbar/m_\Lambda \omega_\Lambda)^{1/2}$, which is used as a simple model calculation [20,36]. Here we choose $b_\Lambda = 2.233$ fm ($\hbar\omega_\Lambda = 7.0$ MeV), simulating the value of the relative r.m.s. distance of $\langle r_\Lambda^2 \rangle^{1/2} = 3.3$-3.6 fm for the $3N$-Λ distribution obtained by four-body ΛNNN calculations using the NN and ΛN potentials [14,37,38]; we have $\langle r_\Lambda^2 \rangle^{1/2} = 3.23$ fm for the HO. The relative $3N$-Λ wave function with $\ell_\Lambda = 0$ for the HO is written as

$$\varphi^{(\Lambda)}_{\ell_\Lambda}(\boldsymbol{r}) = \left(\frac{4}{\tilde{b}_\Lambda^3 \sqrt{\pi}}\right)^{1/2} \exp\left(-\frac{r^2}{2\tilde{b}_\Lambda^2}\right) Y_0^0(\hat{r}), \quad (17)$$

where the size parameter with the c.m. correction is denoted

$$\tilde{b}_\Lambda = b_\Lambda\sqrt{1 + m_\Lambda/3m_N} = 2.634 \text{ fm}, \quad (18)$$

where m_Λ and m_N are the masses of a Λ hyperon and a nucleon, respectively. We confirm $\langle r_\Lambda^2 \rangle^{1/2} = \tilde{b}_\Lambda\sqrt{3/2} = 3.23$ fm for the HO. Figure 4 also shows the $3N$-Λ distribution for the HO taking into account the c.m. correction, which is absolutely essential in light nuclei. We expect that the difference among the $3N$-Λ distributions obtained from several models in Fig. 4 is clearly observed in production cross sections of nuclear (π, K) reactions making a large momentum transfer to the Λ final state. On the other hand, we confirm that the $3N$-N distribution for the HO using the size parameter $b_N = 1.329$ fm ($\hbar\omega_\Lambda = 23.5$ MeV) is in good agreement with that obtained from the C3G potential; the relative r.m.s. distance between $3N$ and N is $\langle r_N^2 \rangle^{1/2} = \tilde{b}_N\sqrt{3/2} = 1.88$ fm, which is quite close to the 1.87 fm for C3G, where $\tilde{b}_N = b_N\sqrt{4/3} = 1.535$ fm.

D. Differential cross sections

We consider the differential laboratory cross sections of the hypernuclear bound state with J^π on a closed-shell target nucleus with $J_A^\pi = 0^+_{\text{g.s.}}$ like ^{4}He, adapting the effective number technique into the DWIA [24,27–30]. Substituting Eqs. (15), (10), and (27) into Eq. (7), we obtain

$$\left(\frac{d\sigma}{d\Omega_K}\right)^{J^\pi}_{\text{lab},\theta_{\text{lab}}} = \alpha\left\langle\frac{d\sigma}{d\Omega_K}\right\rangle^{\text{opt}}_{\pi N \to K\Lambda} N_{\text{eff}}^{J^\pi}(\theta_{\text{lab}}), \quad (19)$$

where $\alpha\langle d\sigma/d\Omega_K\rangle^{\text{opt}}_{\pi N \to K\Lambda}$ is the optimal Fermi-averaged $\pi N \to K\Lambda$ laboratory cross section, as discussed in Sec. II B. The effective number of nucleons $N_{\text{eff}}^{J^\pi}$ for Λ production of the J^π final state in the LS-coupling scheme is written as

$$N_{\text{eff}}^{J^\pi}(\theta_{\text{lab}}) = C_B^2(2L+1)(2\ell_\Lambda+1)\begin{pmatrix}\ell_\Lambda & L & \ell_N \\ 0 & 0 & 0\end{pmatrix}^2|F(q)|^2, \quad (20)$$

where $\ell_\Lambda + L + \ell_N$ must be even due to the non-spin-flip reaction. Thus, only natural-parity states with $J^\pi = 0^+, 1^-, 2^+, 3^-, \ldots$ for the $3N + \Lambda$ systems can be populated. C_B is the isospin-spin spectroscopic amplitude between the Λ final state of $^4_\Lambda$He and the initial state of ^{4}He, which is given by

$$C_B = \left\langle X^B_{T_B,S_B}\Big|\sum_{j=1}^A \hat{O}_j\Big|X^A_{T_A,S_A}\right\rangle. \quad (21)$$

The form factor $F(q)$ in Eq. (20) is given as

$$F(q) = \int_0^\infty r^2 dr \rho^{(\text{tr})}_{\ell_\Lambda \ell_N}(r)\tilde{j}_L\left(q; \frac{M_C}{M_A}r\right), \quad (22)$$

with the $N \to \Lambda$ transition densities

$$\rho^{(\text{tr})}_{\ell_\Lambda \ell_N}(r) = \varphi^{(\Lambda)*}_{\ell_\Lambda}(r)\varphi^{(N)}_{\ell_N}(r) \quad (23)$$

and the distorted waves $\tilde{j}_L(q;z)$, considering the nuclear distortions by mesons in the DW approximation, as we express in Eq. (28); M_C/M_A is the so-called recoil factor for the momentum transfer q. Here we have approximated to

$M_C/M_A \approx M_C/M_B$ in Eq. (7). For $J^\pi = 0^+_{\text{g.s.}}$ in $^4_\Lambda$He, we take $\ell_\Lambda = \ell_N = L = 0$ and $C_B = \sqrt{2}$ in Eq. (20), then we obtain

$$N_{\text{eff}}^{0^+}(\theta_{\text{lab}}) = 2|F(q)|^2, \quad (24)$$

which is expected to observe the hypernuclear fine structure because $F(q)$ is generally sensitive to the nature of the distribution of $\rho^{(\text{tr})}_{00}(r)$, as a function of q.

E. Meson distorted waves

Full distorted waves of the π nucleus and the K nucleus are important to reproduce the absolute values of the cross sections. Because the (π, K) reaction requires a large momentum transfer with a high angular momentum, we simplify the computational procedure in the eikonal approximation to the distorted waves of the meson-nucleus states [20,24,27,28],

$$\chi_K^{(-)*}(\boldsymbol{p}_K, \boldsymbol{r})\chi_\pi^{(+)}(\boldsymbol{p}_\pi, \boldsymbol{r}) = \exp(i\boldsymbol{q}\cdot\boldsymbol{r})D(\boldsymbol{b}, z), \quad (25)$$

with

$$D(\boldsymbol{b}, z) = \exp\left(-\frac{\sigma_\pi(1 - i\alpha_\pi)}{2}\int_{-\infty}^z \rho(\boldsymbol{b}, z')dz' - \frac{\sigma_K(1 + i\alpha_K)}{2}\int_z^\infty \rho(\boldsymbol{b}, z')dz'\right), \quad (26)$$

where σ_π (σ_K) is the averaged total cross section in πN (KN) elastic scatterings, and α_π (α_K) is the ratio of the real and imaginary parts of the corresponding forward scattering amplitudes; $\boldsymbol{b}$ is the impact parameter. $\rho(\boldsymbol{r}) \equiv \rho(\boldsymbol{b}, z)$ is a matter-density distribution fitting to the data on the nuclear charge density [39]. We assume $\alpha_\pi = \alpha_K = 0$, which hardly affects the following results, and we study $\sigma_\pi = 20\text{-}30$ mb and $\sigma_K = 10\text{-}30$ mb [20,24]; $(\sigma_\pi, \sigma_K) = (30 \text{ mb}, 15 \text{ mb})$ is chosen as a standard value [23]. Reducing the right-hand side of Eq. (25) by partial-wave expansion, we obtain

$$\chi_K^{(-)*}(\boldsymbol{p}_K, \boldsymbol{r})\chi_\pi^{(+)}(\boldsymbol{p}_\pi, \boldsymbol{r}) = \sum_L \sqrt{4\pi(2L+1)}i^L\tilde{j}_L(q;r)Y_L^0(\hat{\boldsymbol{r}}) \quad (27)$$

with

$$\tilde{j}_L(q;r) = \sum_{\ell\ell'}i^{\ell-L}\frac{2\ell+1}{2L+1}\sqrt{2\ell'+1}(\ell 0\ell'0|L0)^2 j_\ell(qr)D_{\ell'}(r), \quad (28)$$

where $D_\ell(r)$ is a distortion function [23] defined as

$$D_\ell(r) = \frac{2\ell+1}{2}\int_{-1}^1 D(\boldsymbol{b}, z)P_\ell(\cos\theta)d(\cos\theta). \quad (29)$$

Here $z = r\cos\theta$, $r^2 = \boldsymbol{b}^2 + z^2$, and $P_\ell(x)$ is a Legendre polynomial. If the distortion is switched off, $\tilde{j}_L(q;r)$ is equal to $j_L(qr)$, which is a spherical Bessel function with L.

The production probability for $0^+_{\text{g.s.}}$ in $^4_\Lambda$He is expected to be only 10^{-2}, which is roughly estimated as $\exp(-(bq)^2/2)$ with $bq \simeq 3$ [20], due to the $0s_N \to 0s_\Lambda$ transition with $\Delta L = 0$ in nuclear (π, K) reactions because the Λ continuum states can be populated predominantly by the large angular momentum transfer. Figure 5 displays the distorted waves $\tilde{j}_0(q;r)$ for π
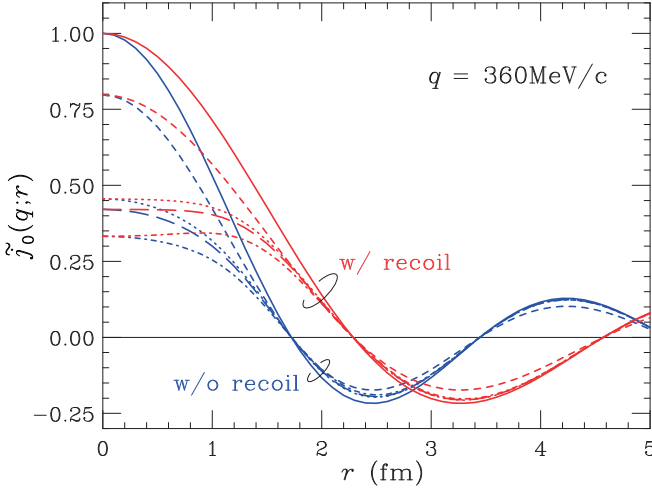
FIG. 5. Distorted waves $\widetilde{j}_L(q;r)$ with $L = 0$ for π and K in the ^{4}He(π, K) reaction at $p_\pi = 1.05$ GeV/c ($\theta_{\mathrm{lab}} = 0°$), which leads to $q = 360$ MeV/c. Solid and dashed curves denote the distorted and the plane waves with/without recoil effects, respectively, as a function of the radial distance between the mesons and the center of the nucleus. Dotted curves denote the waves in the eikonal-oscillator approximation with $\bar{\sigma} = 30$ mb.

and K in the ^{4}He(π, K) reactions at $p_\pi = 1.05$ GeV/c ($\theta_{\mathrm{lab}} = 0°$), which leads to $q = 360$ MeV/c. We find that the values of $\widetilde{j}_0(q;r)$ are reduced near the center of the nucleus due to the nuclear absorption in the distorted wave, in comparison with the plane waves which are obtained with $(\sigma_\pi, \sigma_K) = (0$ mb, 0 mb$)$. We also find that $\widetilde{j}_0(q;r)$ spread outside by taking into account the recoil effects, which bring us to use the *effective momentum transfer*

$$q_{\mathrm{eff}} = \frac{M_C}{M_A}q$$
$$\simeq \frac{A-1}{A}q = \frac{3}{4} \times 360 = 271 \text{ MeV}/c \qquad (30)$$

in the $A = 4$ hypernuclei, as listed in Table I. We recognize a node in $\widetilde{j}_0(q;r)$ at $r = r_n$ satisfied as

$$\frac{M_C}{M_A}qr_n = n\pi \quad (n = 1, 2, \dots), \qquad (31)$$

so we have the point of $r_1 = (M_A/M_C)\pi/q = 2.29$ fm located on the outside of the nucleus having $\langle r_N^2 \rangle^{1/2} = 1.88$ fm for ^{4}He. If we omit the recoil effects $(M_C/M_A \to 1)$, we have $r_1 \to \pi/q = 1.72$ fm, which is located on the inside of the nucleus. Therefore, the recoil effects must be taken into account for the light nuclear target in the (π, K) reactions providing the large momentum transfer to the Λ final state, as we discuss in Sec. III C.

III. RESULTS AND DISCUSSION

Let us consider the Λ production for $0^+_{\mathrm{g.s.}}$ in $^4_\Lambda$He via the (π, K) reactions on the ^{4}He target at $p_\pi = 1.05$ GeV/c in the K forward direction. We discuss the meson distortion effects, comparing the differential laboratory cross sections in the PWIA versus the DWIA, and we study the sensitivity of

TABLE II. Calculated PWIA and DWIA results of the differential laboratory cross sections of $0^+_{\mathrm{g.s.}}$ in $^4_\Lambda$He via the ^{4}He(π^+, K^+) reaction at $p_\pi = 1.05$ GeV/c. The Isle, SG, and HO ($\hbar\omega_\Lambda = 7.0$ MeV) potentials are used with $(\sigma_\pi, \sigma_K) = (30$ mb, 15 mb$)$. Recoil effects are taken into account.

θ_{lab} (deg)	$N_{\mathrm{eff}}^{\mathrm{PW}}$ ($\times 10^{-2}$)	$(d\sigma/d\Omega)_{\mathrm{lab}}^{\mathrm{PW}}$ (μb/sr)	D_{dis}[a]	$N_{\mathrm{eff}}^{\mathrm{DW}}$ ($\times 10^{-2}$)	$(d\sigma/d\Omega)_{\mathrm{lab}}^{\mathrm{DW}}$ (μb/sr)
			Isle		
0	7.571	35.14	0.334	2.527	11.73
4	6.951	33.88	0.324	2.254	10.99
8	5.390	25.25	0.296	1.595	7.47
12	3.540	14.72	0.248	0.879	3.65
			SG		
0	12.68	58.84	0.332	4.211	19.55
4	11.82	57.62	0.325	3.841	18.72
8	9.616	45.06	0.303	2.918	13.67
12	6.876	28.58	0.268	1.846	7.67
			HO		
0	5.160	23.95	0.309	1.595	7.40
4	4.704	22.93	0.298	1.402	6.83
8	3.574	16.75	0.265	0.948	4.44
12	2.281	9.481	0.211	0.482	2.00

[a]$D_{\mathrm{dis}} = N_{\mathrm{eff}}^{\mathrm{DW}}/N_{\mathrm{eff}}^{\mathrm{PW}}$.

the cross sections to the Λ wave functions using the effective number technique of Eq. (19).

A. Differential cross sections for $0^+_{\mathrm{g.s.}}$ in $^4_\Lambda$He

1. PWIA vs DWIA

In Table II, we list the calculated PWIA and DWIA results of the differential laboratory cross sections for $0^+_{\mathrm{g.s.}}$ in $^4_\Lambda$He at $p_\pi = 1.05$ GeV/c in the K forward-direction angles of $\theta_{\mathrm{lab}} = 0°$-$12°$. The differential laboratory cross section of $0^+_{\mathrm{g.s.}}$ in $^4_\Lambda$He accounts for

$$\left(\frac{d\sigma}{d\Omega_K}\right)_{\mathrm{lab},0°}^{J^\pi=0^+} = 35.14 \ \mu\text{b/sr} \quad \text{(PWIA)} \qquad (32)$$

at $p_\pi = 1.05$ GeV/c ($\theta_{\mathrm{lab}} = 0°$), using the Isle potential. When we take into account the distortion with $(\sigma_\pi, \sigma_K) = (30$ mb, 15 mb$)$, we obtain the differential laboratory cross section of $0^+_{\mathrm{g.s.}}$ in $^4_\Lambda$He as

$$\left(\frac{d\sigma}{d\Omega_K}\right)_{\mathrm{lab},0°}^{J^\pi=0^+} = 11.73 \ \mu\text{b/sr} \quad \text{(DWIA)}. \qquad (33)$$

We confirm that the differential laboratory cross sections in DWIA are relatively reduced by a distortion factor which is defined as

$$D_{\mathrm{dis}} \equiv N_{\mathrm{eff}}^{\mathrm{DW}}/N_{\mathrm{eff}}^{\mathrm{PW}} \simeq 0.3, \qquad (34)$$

as listed in Table II. We find that the absolute values of the differential laboratory cross sections for SG (HO) are larger (smaller) than those for Isle. This is because the overlaps of wave functions between N and Λ are larger inside the nucleus in the order SG, Isle, HO, as shown in Fig. 4.
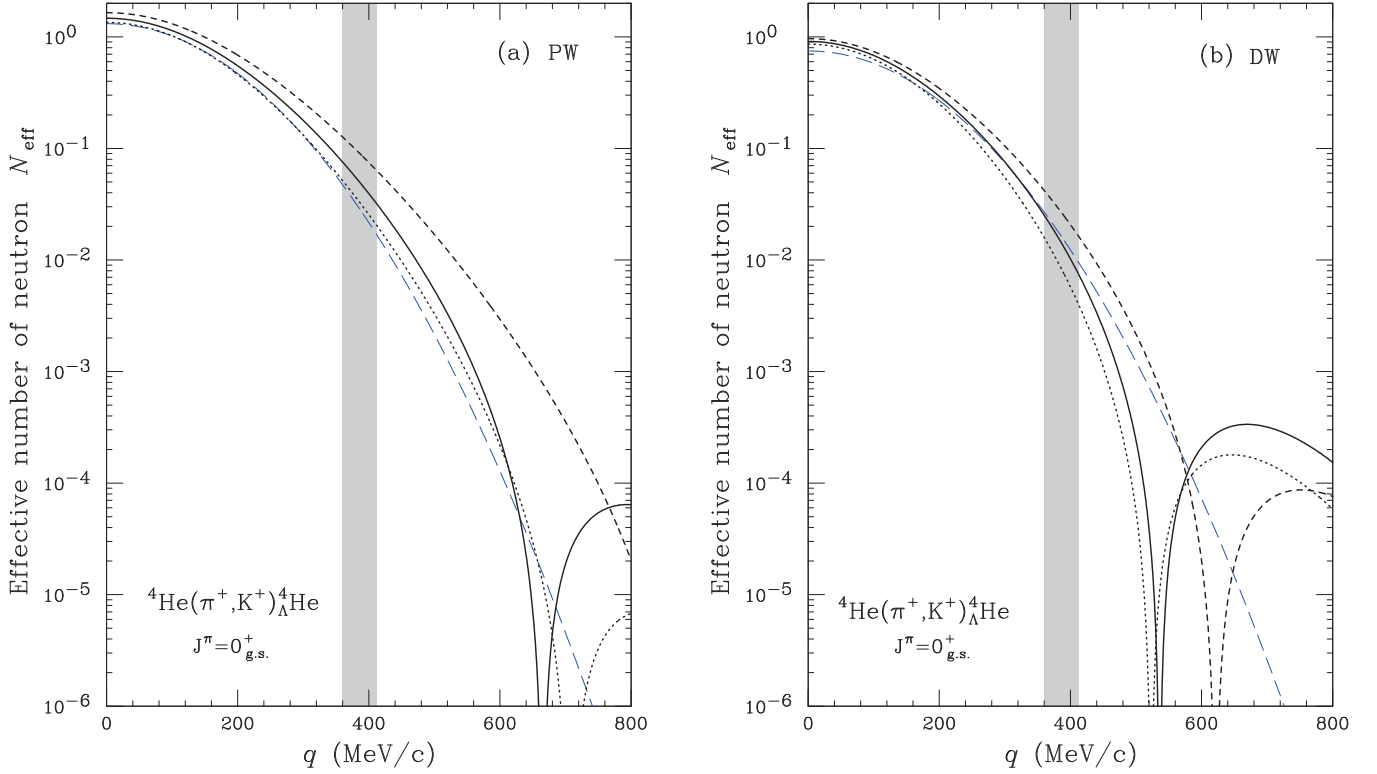
FIG. 6. Calculated effective number of nucleons $N_{eff}^{0^+}$ for $0_{g.s.}^+$ in $^4_\Lambda$He via the ^{4}He(π^+, K^+) reaction with (a) the plane-wave (PW) and (b) the distorted-wave (DW) approximations, as a function of the momentum transfer q. Solid, dashed, and dotted curves denote the results obtained from the Isle, SG, and HO potentials, respectively. Long-dashed curves denote the results in the eikonal-oscillator approximation with $\bar{\sigma} = 30$ mb. The half-tones denote the region of $q = 360\text{-}410$ MeV/c corresponding to $\theta_{lab} = 0°\text{-}12°$ at $p_\pi = 1.05$ MeV/c.

2. $N_{eff}^{0^+}$ vs q

To see the features of the Λ production of the nuclear (π, K) reactions, we study the effective number of nucleons, $N_{eff}^{J^\pi}$, as a function of the momentum transfer q, which is determined by the incident laboratory momentum p_π and the K forward-direction angles of θ_{lab}.

Figure 6(a) displays the calculated results of $N_{eff}^{0^+}$, using the Λ wave functions obtained from the Isle, SG, and HO potentials. The essential physical features of the endothermic nuclear (π, K) reactions can be well understood in terms of $N_{eff}^{0^+}$ in PWIA, as suggested by Dover *et al.* [20]. We confirm that the magnitudes of $N_{eff}^{0^+}$ obtained from the SG, Isle, and HO potentials in PWIA are large in this order. Note that the nuclear (π, K) reactions at $p_\pi = 1.05$ GeV/c ($\theta_{lab} = 0°\text{-}12°$) provide $q = 360\text{-}410$ MeV/c, corresponding to the region of the halftones drawn in Fig. 6, where the recoil effects are very important owing to $q_{eff} \simeq 0.75q$ in $^4_\Lambda$He. On the other hand, exothermic nuclear $(\bar{K}, \pi)$ reactions with $p_\pi = 0.79$ GeV/c ($\theta_{lab} = 0°\text{-}12°$) have $q = 68\text{-}126$ MeV/c, which denote small momentum transfers, thus the recoil effects do not so affect the differential laboratory cross sections. In the region of $q > 600$ MeV/c, we find that the values of $N_{eff}^{0^+}$ obtained from the Isle potential fall off, and their slopes are steeper than those with the SG potential; a dip appears in the region of $q = 600\text{-}800$ MeV/c. This behavior is well known to come from high-momentum components in the ΛN and NN wave functions due to short-range correlations, as discussed in Ref. [19]. We

also find a dip in $N_{eff}^{0^+}$ for HO which includes only the NN correlations.

Figure 6(b) shows the calculated results for $N_{eff}^{0^+}$ with the DWIA. The distortions reduce the magnitudes of $N_{eff}^{0^+}$ by about three times (see Table II), changing slightly the shapes of $N_{eff}^{0^+}$ in the region of $q < 400$ MeV/c. The slopes of $N_{eff}^{0^+}$ become gradually steeper with increasing q as in the case of $q > 400$ MeV/c, and they develop a dip in the region of $q = 520\text{-}620$ MeV/c which can be achieved by $\theta_{lab} = 24°\text{-}34°$. These behaviors may originate from high-momentum components generated by meson distortions, because $D_0(r)$ significantly modifies $j_0(qr)$ inside the nucleus. Therefore, the distortion effects as well as the recoil effects are very important for large momentum transfer processes which can be realized in the (π, K) reactions.

B. Comparison with the eikonal-oscillator approximation

We also consider the differential laboratory cross sections using the single-particle harmonic oscillator wave functions and the eikonal distortions by mesons, referring to this as the "eikonal-oscillator approximation" [20]. This is often employed in nuclear model calculations for several reactions [28,36]. When we use the HO wave functions for both the nucleon and Λ, we can express the eikonal distorted waves as

$$\chi_K^{(-)*}(\boldsymbol{p}_K, \boldsymbol{r})\chi_\pi^{(+)}(\boldsymbol{p}_\pi, \boldsymbol{r}) = \exp(iqz)\exp\left(-\frac{\bar{\sigma}}{2}T(\boldsymbol{b})\right) \quad (35)$$

at the K forward-direction angle of $\theta_{\text{lab}} = 0°$; the nuclear thickness function for the $A = Z + N$ target nucleus is defined as

$$T(\boldsymbol{b}) \equiv \int_{-\infty}^{\infty} \rho(\boldsymbol{r}) dz, \quad \int T(\boldsymbol{b}) d\boldsymbol{b} = A, \qquad (36)$$

with the averaged total cross section $\bar{\sigma} = (\sigma_\pi + \sigma_K)/2$ for the πN and KN elastic scatterings. Thus we have the effective number of nucleons $N_{\text{eff}}^{J^\pi}$ for $0_{\text{g.s.}}^+$ in Eq. (19), which is rewritten as [20,36]

$$N_{\text{eff}}^{0^+}(\theta_{\text{lab}}) \simeq 2\left(\frac{\bar{b}^6}{\tilde{b}_\Lambda^3 \tilde{b}_N^3}\right) \exp\left(-\frac{1}{2}\left(\bar{b}\frac{M_C}{M_A}q\right)^2\right)|G_0(\bar{\sigma})|^2, \quad (37)$$

where the distorted-wave integral [20,36] is defined by

$$G_0(\bar{\sigma}) = \int_0^\infty 2t \exp(-t^2) \exp\left(-\frac{\bar{\sigma}}{2}T(\bar{b}t)\right) dt,$$
$$G_0(\bar{\sigma} = 0) = 1. \qquad (38)$$

Here the mean HO size parameter is denoted

$$1/\bar{b}^2 = \left(1/\tilde{b}_\Lambda^2 + 1/\tilde{b}_N^2\right)/2. \qquad (39)$$

These formulas provide good insight into the nuclear (π, K) reactions. The total effective number of nucleons $N_{\text{eff}}^{\text{tot}}$ at $\theta_{\text{lab}} = 0°$ is defined by the sum of all contributions of the Λ final states. In the closure approximation, it can be easily written as

$$N_{\text{eff}}^{\text{tot}}(0°) = \sum_{J^\pi} N_{\text{eff}}^{J^\pi}(0°)$$
$$\simeq \frac{N}{A} \int T(\boldsymbol{b}) \exp(-\bar{\sigma} T(\boldsymbol{b})) d\boldsymbol{b}, \qquad (40)$$

so that the values of $N_{\text{eff}}^{\text{tot}}(0°)$ amount to 2.00, 1.22, and 0.99 for $\bar{\sigma} = 0$ mb (PW), 20 mb, and 30 mb, respectively. Figure 6 also displays the values of $N_{\text{eff}}^{0^+}$ calculated in the eikonal-oscillator approximation of Eq. (37). In the case of the PWIA, the magnitude of $N_{\text{eff}}^{0^+}$ is as large as that obtained from the HO potential, and it is smaller than that obtained from the Isle potential. In the case of the DWIA ($\bar{\sigma} = 30$ mb), the magnitude of $N_{\text{eff}}^{0^+}$ is as large as that for Isle, and these slopes are similar to each other in the region of $q < 400$ MeV/c. Thus we obtain $(d\sigma/d\Omega)_{\text{lab}}^{\text{DW}} = 10.41, 9.83, 6.90$, and 3.64 μb/sr at $p_\pi = 1.05$ GeV/c for $\theta_{\text{lab}} = 0°, 4°, 8°$, and $12°$, respectively; they are comparable to $(d\sigma/d\Omega)_{\text{lab}}^{\text{DW}} = 11.73, 10.99, 7.47$, and 3.65 μb/sr for Isle. Because high-momentum components of neither the N and Λ wave functions nor the distorted waves for mesons are included in the eikonal-oscillator approximation, we confirm that the shape of $N_{\text{eff}}^{0^+}$ shows no dip with increasing q.

C. Recoil effects

The recoil effects should be needed in the (π, K) reactions on a very light nuclear target such as ^{4}He; the quantity of the recoil factor $M_C/M_A \simeq 3/4 = 0.75$ characterizes the importance of the recoil effects in the nuclear systems. To see the sensitivity to the recoil effects quantitatively, we demonstrate the differential laboratory cross sections when we omit the recoil effects ($M_C/M_A \to 1$) in Eq. (7) using the Isle, SG, and HO potentials.

TABLE III. Calculated PWIA and DWIA results of the differential laboratory cross sections of $0_{\text{g.s.}}^+$ in $_\Lambda^4$He via the ^{4}He(π^+, K^+) reaction at $p_\pi = 1.05$ GeV/c. The Isle, SG, and HO ($\hbar\omega_\Lambda = 7.0$ MeV) potentials are used with $(\sigma_\pi, \sigma_K) = (30$ mb, 15 mb). Recoil effects are omitted.

θ_{lab} (deg)	$N_{\text{eff}}^{\text{PW}}$ ($\times 10^{-2}$)	$(d\sigma/d\Omega)_{\text{lab}}^{\text{PW}}$ (μb/sr)	D_{dis}	$N_{\text{eff}}^{\text{DW}}$ ($\times 10^{-2}$)	$(d\sigma/d\Omega)_{\text{lab}}^{\text{DW}}$ (μb/sr)
			Isle		
0	0.886	4.113	0.093	0.082	0.382
4	0.756	3.684	0.077	0.058	0.283
8	0.466	2.181	0.034	0.016	0.074
12	0.199	0.829	0.000	0.000	0.000
			SG		
0	2.413	11.23	0.162	0.391	1.813
4	2.154	10.59	0.151	0.325	1.583
8	1.538	7.572	0.119	0.183	0.857
12	0.886	3.683	0.071	0.063	0.263
			HO		
0	0.542	2.520	0.054	0.029	0.136
4	0.463	2.256	0.039	0.018	0.092
8	0.286	1.342	0.010	0.003	0.013
12	0.128	0.530	0.011	0.002	0.006

In Table III, we list the calculated DWIA (PWIA) results of the differential laboratory cross sections omitting the recoil effects via the ^{4}He(π, K) reaction at $p_\pi = 1.05$ GeV/c. We find $(d\sigma/d\Omega)_{\text{lab}} = 0.382$ μb/sr (4.113 μb/sr) at $\theta_{\text{lab}} = 0°$. Surprisingly, this value is an order of magnitude smaller than $(d\sigma/d\Omega)_{\text{lab}} = 11.73$ μb/sr (35.14 μb/sr), which is already listed in Table II. The recoil effects have a great influence on $(d\sigma/d\Omega)_{\text{lab}}$ depending on the radial behavior of the distorted waves for mesons. Here we consider the overlap function defined as

$$\mathcal{Y}(q; r) = r^2 \rho_{00}^{(\text{tr})}(r) \tilde{j}_0\left(q; \frac{M_C}{M_A}r\right), \qquad (41)$$

which corresponds to the integrand in Eq. (22). Figure 7 displays the behaviors of $\mathcal{Y}(q; r)$ for various types choosing the Λ wave functions and the distortion parameters, as a function of the radial distance. When we omit the recoil effects ($M_C/M_A \to 1$), we find that the node point at r_1 where $\mathcal{Y}(q; r_1) = 0$ must be shifted toward the nuclear interior. As a result, the integral value of $\int_0^\infty \mathcal{Y}(q; r) dr = F(q)$ is significantly reduced by cancellation between the positive and the negative values over integration regions in $\mathcal{Y}(q; r)$, as illustrated in Fig. 7.

The recoil effects are often omitted in several model calculations for nuclear reactions with large momentum transfers, e.g., (π, K) [20], $(\bar{K}, K)$ [28], $(\bar{K}, p)$ [36], and (stopped $\bar{K}, \pi$) [40] reactions on ^{12}C in which the recoil effects are not so important because $M_C/M_A \simeq (A - 1)/A = 11/12 = 0.917$ for $A = 12$. But we must pay attention to the recoil effects when applying it to light nuclear systems such as ^{4}He ($M_C/M_A \simeq 3/4 = 0.75$). We believe that the calculated cross sections [28] or calculated production probabilities [40] of $_\Lambda^4$He are perhaps underestimated by an order of magnitude due to the lack of the recoil effects [41].
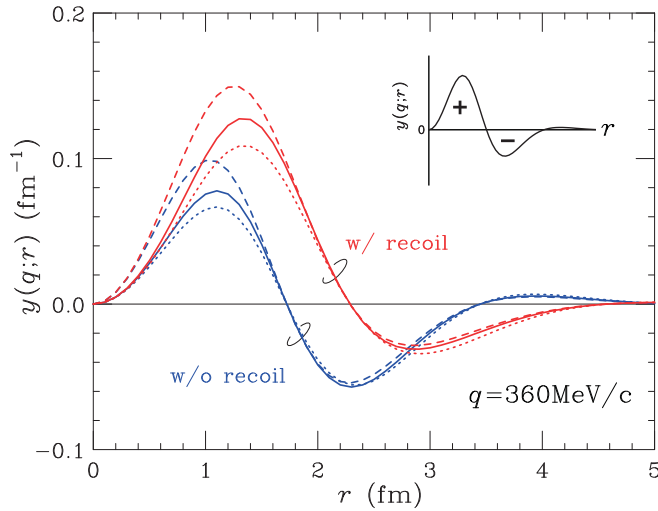
FIG. 7. Overlap functions of $\mathcal{Y}(q;r)$ with/without the recoil effects in the ^{4}He(π, K) reactions at $p_\pi = 1.05$ GeV/c (0°), which leads to $q = 360$ MeV, as a function of the radial distance. Solid, dashed, and dotted curves denote the results obtained from the Isle, SG, and HO potentials, respectively.
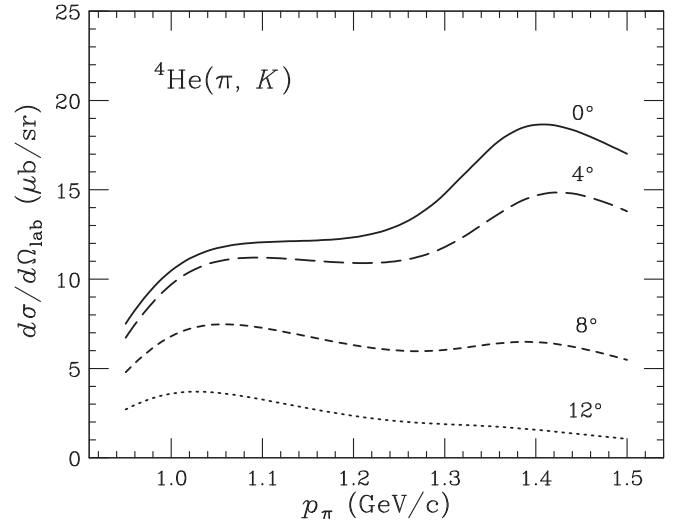

FIG. 8. Incident-momentum dependence of the differential laboratory cross sections in the ^{4}He(π, K) reactions at $\theta_{\text{lab}} = 0°$, 4°, 8°, and 12°, as a function of p_π. The Λ wave functions obtained by the Isle potential and the distortion parameters of $(\sigma_\pi, \sigma_K) = (30$ mb, 15 mb$)$ are used.

D. Dependence on distortion parameters

Due to strong absorptions of mesons in nuclei, e.g., π^+ at $p_\pi = 1.0$-1.5 GeV/c in the N^* resonance region, the magnitude of the cross section may also be affected by meson distortions. To understand the distortion effects quantitatively, we demonstrate the differential laboratory cross sections of $0^+_{\text{g.s.}}$ in $_\Lambda^4$He, considering various eikonal distortions with parameters of (σ_π, σ_K). In Table IV, we show the calculated results of $(d\sigma/d\Omega)_{\text{lab}}$ at $p_\pi = 1.05$ GeV/c. The magnitudes of the cross sections are reduced upon increasing these parameters in the DWIA. Thus the differential laboratory cross sections of $0^+_{\text{g.s.}}$ in $_\Lambda^4$He at $\theta_{\text{lab}} = 0°$ amount to $(d\sigma/d\Omega)_{\text{lab}} \simeq 8$-14 μb/sr, which depend on π and K distorted waves for $\sigma_\pi = 20$-30 mb and $\sigma_K = 10$-30 mb. It should be noted that the parameter

TABLE IV. Distortion-parameter dependence of the differential laboratory cross sections of $0^+_{\text{g.s.}}$ in $_\Lambda^4$He via the ^{4}He(π^+, K^+) reaction at $p_\pi = 1.05$ GeV/c. The Isle potential for Λ is used.

(σ_π, σ_K) (mb)	θ_{lab} (deg)	D_{dis}	$N_{\text{eff}}^{\text{DW}}$ ($\times 10^{-2}$)	$(d\sigma/d\Omega)_{\text{lab}}^{\text{DW}}$ (μb/sr)
(20, 20)	0	0.387	2.932	13.61
	4	0.378	2.629	12.81
	8	0.351	1.889	8.85
	12	0.304	1.075	4.47
(30, 10)	0	0.372	2.818	13.08
	4	0.363	2.523	12.30
	8	0.335	1.805	8.45
	12	0.287	1.016	4.22
(30, 30)	0	0.243	1.841	8.54
	4	0.234	1.625	7.92
	8	0.206	1.110	5.20
	12	0.160	0.568	2.36

dependence gives an indication of the accuracy of our results within the eikonal distortion. Fully realistic distorted waves obtained from meson-nucleus optical potentials would be needed for a more quantitative discussion.

E. Dependence on the incident momentum

In Fig. 8, we display the differential laboratory cross sections of $0^+_{\text{g.s.}}$ in $_\Lambda^4$He via the ^{4}He(π, K) reactions at $\theta_{\text{lab}} = 0°$, 4°, 8°, and 12°, as a function of the incident laboratory momentum p_π. Here we have used the Λ wave functions obtained from the Isle potential and the eikonal distortions with $(\sigma_\pi, \sigma_K) = (30$ mb, 15 mb$)$. We find that the differential laboratory cross sections slightly increase with increasing p_π. This trend seems to be opposite to that of $\alpha \langle d\sigma/d\Omega_{\text{lab}} \rangle_{\pi N \to K\Lambda}^{\text{opt}}$, as shown in Fig. 2. This stems from the fact that the momentum transfers in this region decrease with increasing p_π (see Fig. 1), together with the nature of $N_{\text{eff}}^{0^+}$, which must take into account the recoil effects.

IV. SUMMARY AND CONCLUSION

We have investigated theoretically the production cross sections of the 0^+ ground state of a $_\Lambda^4$He hypernucleus in the ^{4}He(π, K) reaction with a distorted-wave impulse approximation using the optimal Fermi-averaged $\pi N \to K\Lambda$ t matrix. We have demonstrated the sensitivity of the production cross section to the $3N$-Λ potentials and to the eikonal distorted waves for mesons. We have calculated the differential laboratory cross sections of $(d\sigma/d\Omega)_{\text{lab}}$ at $p_\pi = 1.05$ GeV/c in the K forward-direction angles of $\theta_{\text{lab}} = 0°$-12°. The results can be summarized as follows.

1. The calculated differential laboratory cross section of $0^+_{\text{g.s.}}$ in $_\Lambda^4$He amounts to $(d\sigma/d\Omega)_{\text{lab}} \simeq 11$ μb/sr at

$p_\pi = 1.05$ GeV/c, $\theta_{\rm lab} = 0°$-$4°$, as in the case of the Isle potential.

2. The recoil effects enlarge the cross section of $^4_\Lambda$He via the ^{4}He(π, K) reactions by an order of magnitude, whereas the meson distortions reduce the cross section by 30%.

3. It is important to take into account the energy dependence of the $\pi N \to K\Lambda$ cross sections for a good description of the nuclear (π, K) reactions.

4. The differential laboratory cross sections of $^4_\Lambda$H via ^{4}He(π^-, K^0) reactions are the same as those of $^4_\Lambda$He via ^{4}He(π^+, K^+) owing to charge independence in nuclear physics.

In conclusion, we have shown that the differential laboratory cross sections of $0^+_{\rm g.s.}$ in $^4_\Lambda$He amount to $(d\sigma/d\Omega)_{\rm lab} \simeq 11$ μb/sr at $p_\pi = 1.05$ GeV/c in the K forward direction because of the major advantage of the use of s-shell nuclear targets such as ^{4}He. It would be appropriate to study the Λ production from (π, K) reactions on s-shell ^{3,4}He targets in order to study the lifetime measurements of a $^{3,4}_\Lambda$H hypernucleus in production followed by mesonic decay processes. This investigation is now in progress [12].

APPENDIX: EXPLICIT FORMS OF ISOSPIN-SPIN FUNCTIONS FOR $0^+_{\rm g.s.}$ IN ^{4}He AND $^4_\Lambda$He

The isospin-spin function $X^A_{T_A, S_A}$ for $0^+_{\rm g.s.}$ in ^{4}He ($T_A = 0$, $m_{T_A} = 0$; $S_A = 0$, $m_{S_A} = 0$) in Eq. (15) is explicitly written as

$$X^A_{T_A, S_A} = \mathcal{A}\left[\chi^{(3N)}_{I_3, S_3} \otimes \chi^{(N)}_{1/2, 1/2}\right]_{0,0}$$

$$= \frac{1}{2\sqrt{6}}(-p_\uparrow p_\downarrow n_\uparrow n_\downarrow + p_\uparrow p_\downarrow n_\downarrow n_\uparrow + p_\downarrow p_\uparrow n_\uparrow n_\downarrow$$
$$- p_\downarrow p_\uparrow n_\downarrow n_\uparrow + p_\uparrow n_\uparrow p_\downarrow n_\downarrow - p_\uparrow n_\downarrow p_\downarrow n_\uparrow - p_\downarrow n_\uparrow p_\uparrow n_\downarrow$$
$$+ p_\downarrow n_\downarrow p_\uparrow n_\uparrow - p_\uparrow n_\uparrow n_\downarrow p_\downarrow + p_\uparrow n_\downarrow n_\uparrow p_\downarrow + p_\downarrow n_\uparrow n_\downarrow p_\uparrow$$
$$- p_\downarrow n_\downarrow n_\uparrow p_\uparrow - n_\uparrow p_\uparrow p_\downarrow n_\downarrow + n_\uparrow p_\downarrow p_\downarrow n_\uparrow + n_\downarrow p_\uparrow p_\downarrow n_\uparrow$$
$$- n_\downarrow p_\downarrow p_\uparrow n_\uparrow + n_\uparrow p_\uparrow n_\downarrow p_\downarrow - n_\uparrow p_\downarrow n_\downarrow p_\uparrow - n_\downarrow p_\uparrow n_\uparrow p_\downarrow$$
$$+ n_\downarrow p_\downarrow n_\uparrow p_\uparrow - n_\uparrow n_\downarrow p_\uparrow p_\downarrow + n_\uparrow n_\downarrow p_\downarrow p_\uparrow + n_\downarrow n_\uparrow p_\uparrow p_\downarrow$$
$$- n_\downarrow n_\uparrow p_\downarrow p_\uparrow), \tag{A1}$$

where $p_\uparrow$ and $n_\uparrow$ ($p_\downarrow$ and $n_\downarrow$) denote spin states with $m_z = +1/2$ ($-1/2$) for a proton and a neutron, respectively. The isospin-spin function $X^B_{T_B, S_B}$ for $0^+_{\rm g.s.}$ in $^4_\Lambda$He ($T_B = 1/2$, $m_{T_B} = +1/2$; $S_B = 0$, $m_{S_B} = 0$) in Eq. (10) is explicitly written as

$$X^B_{T_B, S_B} = \left[\chi^{(3N)}_{I_3, S_3} \otimes \chi^{(\Lambda)}_{0, 1/2}\right]_{1/2, 0}$$

$$= \frac{1}{2\sqrt{3}}(-p_\uparrow p_\downarrow n_\uparrow \Lambda_\downarrow + p_\uparrow p_\downarrow n_\downarrow \Lambda_\uparrow + p_\downarrow p_\uparrow n_\uparrow \Lambda_\downarrow$$
$$- p_\downarrow p_\uparrow n_\downarrow \Lambda_\uparrow + p_\uparrow n_\uparrow p_\downarrow \Lambda_\downarrow + p_\downarrow n_\downarrow p_\uparrow \Lambda_\uparrow - n_\uparrow p_\uparrow p_\downarrow \Lambda_\downarrow$$
$$+ n_\uparrow p_\downarrow p_\uparrow \Lambda_\downarrow - n_\uparrow p_\downarrow p_\downarrow \Lambda_\uparrow - n_\downarrow p_\uparrow p_\uparrow \Lambda_\downarrow + n_\downarrow p_\uparrow p_\downarrow \Lambda_\uparrow$$
$$- n_\uparrow p_\uparrow p_\downarrow \Lambda_\uparrow), \tag{A2}$$

where $\Lambda_\uparrow$ ($\Lambda_\downarrow$) denotes a spin state with $m_z = +1/2$ ($-1/2$) for a Λ hyperon.

[1] C. Rappold *et al.* (HypHI Collaboration), Nucl. Phys. A **913**, 170 (2013).

[2] J. Adam *et al.* (ALICE Collaboration), Phys. Lett. B **754**, 360 (2016).

[3] L. Adamczyk *et al.* (STAR Collaboration), Phys. Rev. C **97**, 054909 (2018).

[4] S. Trogolo (ALICE Collaboration), Nucl. Phys. A **982**, 815 (2019).

[5] A. Gal and H. Garcilazo, Phys. Lett. B **791**, 48 (2019), and references therein.

[6] H. Kamada, J. Golak, K. Miyagawa, H. Witała, and W. Glöckle, Phys. Rev. C **57**, 1595 (1998).

[7] H. Outa *et al.*, Nucl. Phys. A **639**, 251c (1998).

[8] T. Motoba, Nucl. Phys. A **547**, 115 (1992).

[9] I. Kumagai-Fuse, S. Okabe, and Y. Akaishi, Phys. Lett. B **345**, 386 (1995).

[10] H. Asano *et al.*, $^3_\Lambda$H and $^4_\Lambda$H mesonic weak decay lifetime measurement with ^{3,4}He$(K^-, \pi^0)^{3,4}_\Lambda$H reaction. Proposal for Nuclear and Particle Physics experiments at the J-PARC (2018); http://j-parc.jp/NuclPart/Proposal_e.html.

[11] M. Agnello *et al.*, Direct measurement of the $^3_\Lambda$H and $^4_\Lambda$H lifetimes using the ^{3,4}He$(\pi^-, K^0)^{3,4}_\Lambda$H reactions. Proposal for Nuclear and Particle Physics experiments at the J-PARC (2019); http://j-parc.jp/NuclPart/Proposal_e.html.

[12] T. Harada and Y. Hirabayashi, arXiv:1901.03845 [nucl-th].

[13] A. Gal, E. V. Hungerford, and D. J. Millener, Rev. Mod. Phys. **88**, 035004 (2016).

[14] R. H. Dalitz, R. C. Herndon, and Y. C. Tang, Nucl. Phys. B **47**, 109 (1972).

[15] Y. Akaishi, T. Harada, S. Shinmura, and Khin Swe Myint, Phys. Rev. Lett. **84**, 3539 (2000).

[16] R. H. Dalitz and F. von Hippel, Phys. Lett. **10**, 153 (1964).

[17] A. Gal, Phys. Lett. B **744**, 352 (2015); D. Gazda and A. Gal, Nucl. Phys. A **954**, 161 (2016).

[18] T. Harada, Phys. Rev. Lett. **81**, 5287 (1998); Nucl. Phys. A **672**, 181 (2000).

[19] S. Shinmura, Y. Akaishi, and H. Tanaka, Prog. Theor. Phys. **76**, 157 (1986).

[20] C. B. Dover, L. Ludeking, and G. E. Walker, Phys. Rev. C **22**, 2073 (1980).

[21] T. Harada (unpublished) (2006).

[22] S. Ajimura *et al.*, Exclusive study on the ΛN weak interaction in $A = 4$ Λ-hypernuclei. Proposal for Nuclear and Particle Physics experiments at the J-PARC (2006); http://j-parc.jp/NuclPart/Proposal_e.html.

[23] T. Harada and Y. Hirabayashi, Nucl. Phys. A **759**, 143 (2005); **767**, 206 (2006).

[24] J. Hüfner, S. Y. Lee, and H. A. Weidenmüller, Nucl. Phys. A **234**, 429 (1974).

[25] E. H. Auerbach, A. J. Baltz, C. B. Dover, A. Gal, S. H. Kahana, L. Ludeking, and D. J. Millener, Ann. Phys. (NY) **148**, 381 (1983).

[26] S. Tadokoro, H. Kobayashi, and Y. Akaishi, Phys. Rev. C **51**, 2656 (1995).

[27] T. Koike and T. Harada, Nucl. Phys. A **804**, 231 (2008).

[28] C. B. Dover and A. Gal, Ann. Phys. (NY) **146**, 309 (1983).

[29] O. Morimatsu and K. Yazaki, Nucl. Phys. A **483**, 493 (1988); Prog. Part. Nucl. Phys. **33**, 679 (1994).

[30] K. Itonaga, T. Motoba, O. Richter, and M. Sotona, Phys. Rev. C **49**, 1045 (1994).

[31] M. Sotona and J. Žofka, Prog. Theor. Phys. **81**, 160 (1989).

[32] Y. Kurihara, Y. Akaishi, and H. Tanaka, Prog. Theor. Phys. **67**, 1483 (1982).

[33] Y. Akaishi, *International Review of Nuclear Physics 4* (World Scientific, Singapore, 1986), p. 259.

[34] Y. Kurihara, Y. Akaishi, and H. Tanaka, Phys. Rev. C **31**, 971 (1985).

[35] T. Harada, S. Shinmura, Y. Akaishi, and H. Tanaka, Nucl. Phys. A **507**, 715 (1990).

[36] A. Cieplý, E. Friedman, A. Gal, and J. Mareš, Nucl. Phys. A **696**, 173 (2001).

[37] A. R. Bodmer and Q. N. Usmani, Phys. Rev. C **31**, 1400 (1985).

[38] E. Hiyama, M. Kamimura, T. Motoba, T. Yamada, and Y. Yamamoto, Phys. Rev. C **65**, 011301(R) (2001).

[39] H. de Vries, C. W. de Jager, and C. de Vries, At. Data Nucl. Tables **36**, 495 (1987).

[40] A. Matsuyama and K. Yazaki, Nucl. Phys. A **477**, 673 (1988).

[41] T. Koike and T. Harada, Phys. Lett. B **652**, 262 (2007).